

Cross-Channel Transfer of Linear Momentum in Smooth Rectangular Channels

GEOLOGICAL SURVEY WATER-SUPPLY PAPER 1592-B



PROPERTY OF
U.S. GEOLOGICAL SURVEY
GROUND WATER BRANCH
TRENTON, N.J.

Cross-Channel Transfer of Linear Momentum in Smooth Rectangular Channels

By R. W. CRUFF

LABORATORY STUDIES OF OPEN-CHANNEL FLOW

GEOLOGICAL SURVEY WATER-SUPPLY PAPER 1592-B



UNITED STATES DEPARTMENT OF THE INTERIOR

STEWART L. UDALL, *Secretary*

GEOLOGICAL SURVEY

William T. Pecora, *Director*

CONTENTS

| | Page |
|---|------|
| Symbols..... | iv |
| Abstract..... | B1 |
| Introduction..... | 1 |
| Linear momentum transfer..... | 2 |
| Linear momentum equation..... | 3 |
| Review of the literature..... | 5 |
| Apparatus and procedures..... | 7 |
| The flume..... | 7 |
| Depth measurements..... | 8 |
| Velocity measurements..... | 8 |
| Results..... | 9 |
| Shear-stress analysis..... | 10 |
| Distribution of the shear stress..... | 11 |
| Maximum shear stress..... | 18 |
| Average shear stress..... | 21 |
| Apparent shear force..... | 23 |
| Cross-channel transfer of momentum..... | 24 |
| Summary..... | 24 |
| References cited..... | 25 |

ILLUSTRATIONS

| | Page |
|---|------|
| FIGURE 1. Definition sketch of forces in the momentum equation..... | B4 |
| 2. Channel cross sections..... | 7 |
| 3. Typical surface profiles..... | 9 |
| 4. Typical vertical velocity traverse (central region)..... | 11 |
| 5-12. Shear-stress distribution, bottom: | |
| 5. $(0.026 < y_0/B < 0.030)$ | 12 |
| 6. $(0.040 < y_0/B < 0.050)$ | 12 |
| 7. $(0.050 < y_0/B < 0.062)$ | 13 |
| 8. $(0.074 < y_0/B < 0.087)$ | 13 |
| 9. $(0.110 < y_0/B < 0.120)$ | 14 |
| 10. $(0.140 < y_0/B < 0.145)$ | 14 |
| 11. $(0.195 < y_0/B < 0.215)$ | 15 |
| 12. (Lane, 1955)..... | 15 |
| 13-17. Shear-stress distribution, wall: | |
| 13. $(0.026 < y_0/B < 0.030)$ | 16 |
| 14. $(0.040 < y_0/B < 0.062)$ | 16 |
| 15. $(0.074 < y_0/B < 0.087)$ | 17 |
| 16. $(0.110 < y_0/B < 0.120)$ | 17 |
| 17. $(0.140 < y_0/B < 0.215)$ | 18 |

| | Page |
|--|---------|
| FIGURE 18, 19. Maximum shear stress, bottom..... | B19, 20 |
| 20, 21. Maximum shear stress, wall..... | 20, 21 |
| 22. Average shear stress..... | 22 |
| 23. Average boundary shear stress..... | 22 |
| 24, 25. Apparent shear force..... | 23, 24 |

TABLE

| | Page |
|-------------------------------|------|
| TABLE 1. Summary of data..... | B10 |

SYMBOLS

| | |
|------------------|--|
| a | Constant. |
| A | Area of cross section. |
| b | One-half the total width of channel bottom, $\frac{1}{2}B$. |
| B | Total width of channel bottom. |
| F_a | Apparent shear force. |
| F'_a | Apparent shear force for incremental distance in the longitudinal direction. |
| p | Pressure. |
| P | Wetted perimeter. |
| R | Hydraulic radius, A/P . |
| R | Reynolds number. |
| S_0 | Slope of the uniform flow. |
| u | Velocity at a point. |
| u_* | Local shear velocity, $\sqrt{\tau_0/\rho}$. |
| \bar{u}_* | Average shear velocity, $\sqrt{\bar{\tau}_0/\rho}$. |
| \bar{U} | Average velocity in the cross section. |
| y | Distance above the channel bottom. |
| y_0 | Uniform flow depth. |
| z | Distance from the wall in the lateral direction. |
| β | Correction for the variation in shear stress along the solid boundary. |
| γ | Specific weight of fluid. |
| $\bar{\epsilon}$ | Correction for the apparent shear at the free surface of an open channel. |
| θ | Slope angle. |
| κ | Von Kármán's constant. |
| ν | Kinematic viscosity. |
| ρ | Fluid mass density. |
| τ_0 | Local boundary shear stress. |
| $\bar{\tau}_a$ | Average apparent shear stress. |
| $\bar{\tau}_0$ | Average boundary shear stress. |
| τ'_0 | Two-dimensional shear stress, $\gamma y_0 S_0$. |

SUBSCRIPTS, UNLESS OTHERWISE DEFINED ABOVE

| | |
|-----|-------------------------|
| b | Bottom. |
| w | Wall. |
| x | Longitudinal direction. |
| y | Vertical direction. |
| z | Lateral direction. |
| 1 | Upstream section. |
| 2 | Downstream section. |

SUPERSCRIPT, UNLESS OTHERWISE DEFINED ABOVE

| | |
|-----|---------------|
| $-$ | Time average. |
|-----|---------------|

LABORATORY STUDIES OF OPEN-CHANNEL FLOW

CROSS-CHANNEL TRANSFER OF LINEAR MOMENTUM IN SMOOTH RECTANGULAR CHANNELS

By R. W. CRUFF

ABSTRACT

The object of this investigation was to study the lateral transfer of momentum from the central region to the vertical-wall regions in smooth rectangular channels. The first step in the method was to determine the shear stress along the channel periphery. This shear stress was then incorporated in the momentum equation to solve for the lateral cross-channel transfer of linear momentum.

The shear stress along the channel periphery was computed by two methods: one made use of the Preston-tube technique, and the other, the Kármán-Prandtl logarithmic velocity law. From these computed shear stresses the shear-stress distributions, the maximum shear stress, and the average shear stresses for the channel bottom and walls were determined and plotted. The average shear stress for the channel bottom was much larger than that for the channel walls at the small depth-to-width ratios. The difference became less at the larger depth-to-width ratios. The depth-to-width ratio of the channel cross section was the only flow characteristic which affected the boundary shear stress (distribution, maximum, and average) for smooth boundaries and for a moderate range of Reynolds numbers. A central region in which shear stress was approximately equivalent to the shear stress for two-dimensional flow was found by the writer for smooth rectangular channels whose depth-to-width ratios were less than 0.08. In other words, for smooth rectangular channels the region in which the shear stress is affected by the wall extends a distance of about six times the flow depth laterally from the wall.

INTRODUCTION

Except for the effects of the free surface, the laws which govern the motion of fluids in closed conduits are equally applicable to uniform open-channel flow. Rapid advances have been made in recent years on the problem of flow in circular closed conduits. Similar progress has not been made in the field of open-channel flow because of additional complexities created by the presence of the free surface and by the normally asymmetrical cross section. Comparatively few systematic investigations have been made of open channels since the monumental work of Bazin, over a century ago.

The experimental data for this report were collected during an earlier study and have been reported in part by Tracy and Lester (1961). The project was conducted in the hydraulics laboratory of the Georgia Institute of Technology, under a cooperative agreement between the U.S. Geological Survey and the Georgia Institute of Technology. The analysis for this report was performed under the direction of Dr. M. R. Carstens, Professor of Civil Engineering at Georgia Institute of Technology.

The objective of this investigation was an analysis of the data; special study was made of the cross-channel transfer of linear momentum. The writer's analysis was based on a study of the shear-stress distribution along the channel bottom and walls.

LINEAR MOMENTUM TRANSFER

All shear flows are characterized by a net transfer of longitudinal linear momentum from regions of higher linear momentum to regions of lower linear momentum.

The simplest example is that of laminar flow in a pipe. In such flow, linear momentum is transported toward the wall region by a molecular transfer. Where flow in a pipe is turbulent, the linear momentum is transferred to the wall region by the movement of microscopic masses of fluid.

Another example is that of overbank flow. In this type of flow, linear momentum is transported from the main channel section to the overbank section both by turbulence and by vertically oriented giant eddies (at least with shallow depths in the overbank section) which form at the junction plane of the main channel and overbank sections. The existence of these vertically oriented giant eddies was observed by Wilroy (1953) and Rodriguez-Diaz (1954) in their studies of the hydraulic jump in a nonrectangular open channel. The channel studied by Wilroy and Rodriguez-Diaz had vertical walls and a cross-channel slope of the bottom; the depth across the channel was therefore variable. For a hydraulic jump to occur in such a channel, a massive transfer of linear momentum from the deeper to the shallower part is required. Rodriguez-Diaz observed that, under certain conditions, turbulence plus steady cross currents were sufficient to effect the required transfer. On the other hand, if the required rate of transfer was too great, vertically oriented giant eddies formed which were capable of massive transport of linear momentum toward the shallower side.

Another mechanism which can transport linear momentum consists of line vortices alined with axes along the channel. The superposition of these line vortices on the flow is called secondary circulation. Prandtl (1952) presented a hypothesis about the location of these

vortex pairs in various noncircular conduits. This secondary circulation is an effective supplément to turbulence in transferring linear momentum toward the wall regions in flow in noncircular conduits.

In a rectangular open channel, linear momentum must be transferred both downward toward the floor and laterally toward the walls. The lateral transport is necessitated by the existence of boundary shear on the walls. Where flow is two dimensional the net transport is in only one direction—toward the floor. Conceptually the flow is divided into two three-dimensional flow regions near the walls and into a two-dimensional flow region in the central part of the channel. The mean and the fluctuating velocity patterns in a two-dimensional region have been studied by Laufer (1951), who conducted experiments using a rectangular smooth conduit. The existence of a three-dimensional flow region near the wall is reflected in the following flow characteristics: Mean velocity, turbulence, apparent shear stresses, and boundary shear stress.

Boundary shear stress is a flow characteristic of major interest to engineers. For example, most engineering analyses are based on a gross-streamtube analysis, for which the total boundary shear force is generally required. As a further example, movement of particles on the bed and on the banks of a stream is directly related to the boundary shear stress. Determination of the boundary shear-stress distribution and the cross-channel transfer of linear momentum in rectangular open channels was the object of this investigation.

LINEAR MOMENTUM EQUATION

The linear momentum equation for steady flow is simply:

$$\left[\begin{array}{c} \text{Summation of the} \\ \text{external forces} \\ \text{on a free body} \end{array} \right] = \left[\begin{array}{c} \text{Rate of transport} \\ \text{of linear momentum} \\ \text{out of the free body} \end{array} \right] - \left[\begin{array}{c} \text{Rate of transport} \\ \text{of linear momentum} \\ \text{into the free body} \end{array} \right] \quad (1)$$

For purpose of analysis a rectangular parallelepiped (fig. 1) was chosen as a fluid free body. Face 1 is at the junction of the fluid and the bed. Face 2 is the free surface. Face 3 is a vertical plane along the centerline. Face 4 is a vertical plane parallel to the centerline at a distance of $b-z$ from the centerline. Faces 5 and 6 are the end faces of the free body and are separated by the axial distance dx . The linear momentum equation in the x -direction, along the axis of the channel, is formulated for steady uniform flow.

The external forces in the x -direction on the free body are: (a) The pressure forces on faces 5 and 6; (b) the boundary shear force on face 1, $dx \int_b^z \tau_{0b}(-dz)$; and (c) the weight force, $\gamma(b-z)(y_0 \sin \theta)dx$. Because the flow is uniform the pressure force on face 5 exactly equals that on face 6.

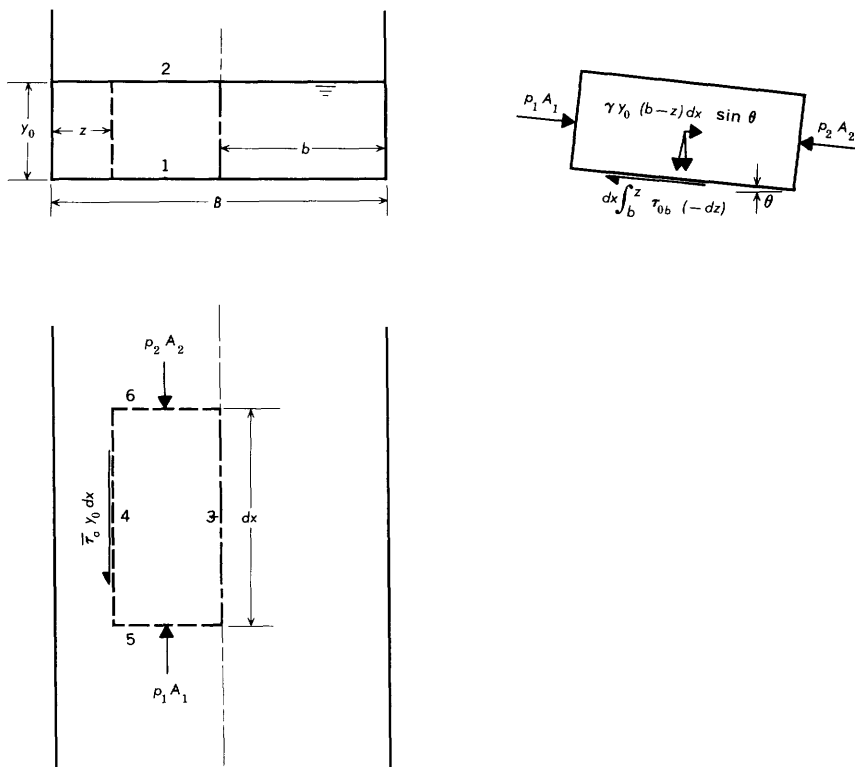


FIGURE 1.—Definition sketch of forces in the momentum equation.

The linear momentum transport terms are as follows:

1. The linear momentum transport rate out through face 6 exactly equals the transport rate in through face 5.
2. The net transport rate of linear momentum through face 3 by turbulent eddies is zero, because of the location of face 3 on the axis of symmetry.
3. The linear momentum transport rate out through face 4 is affected both by turbulent eddies and by secondary circulation.

The traditional treatment of the term for the rate of transport of linear momentum out through face 4 is to transfer it to the left side of equation 1. After this transfer is performed, the term can be considered as representing apparent shear force, $\bar{\tau}_a y_0 dx$.

The linear momentum equation is:

$$-dx \int_b^* \tau_{0b} (-dz) - \bar{\tau}_a y_0 dx + \gamma_a (b-z) (y_0 \sin \theta) dx = 0 \quad (2)$$

in which

b = one-half the total channel width

x = distance in the longitudinal direction

y_0 = uniform flow depth

z = distance laterally from the wall

γ = fluid specific weight

θ = slope angle

τ_{0b} = shear stress on the channel bottom

$\bar{\tau}_a$ = average apparent shear stress

For the entire channel—that is, $z=0$ —equation 2 reduces to:

$$-\bar{\tau}_{0b}(b)dx - \bar{\tau}_{0w}y_0dx + \gamma(b)(y_0 \sin \theta)dx = 0$$

in which $\bar{\tau}_{0b}$ is the mean shear stress on the bed and $\bar{\tau}_{0w}$ is the mean shear stress on the wall. Equation 2 simplified is

$$-\bar{\tau}_{0b}(B) - \bar{\tau}_{0w}(2y_0) + \gamma(By_0)S_0 = 0 \quad (3)$$

in which S_0 is the bottom slope, $\sin \theta$. The common procedure is to obtain the mean value over the entire boundary rather than averaging the bottom and walls separately. Hence equation 3 can be simplified as follows:

$$-\tau_0(B + 2y_0) + \gamma(By_0)S_0 = 0$$

or

$$\bar{\tau}_0 = \gamma(A/P)S_0 = \gamma RS_0 \quad (3a)$$

in which $\bar{\tau}_0$ is the mean shear stress averaged over the entire boundary; A is the cross-sectional area, By_0 ; P is the wetted perimeter, $B + 2y_0$; and R is the hydraulic radius, A/P .

REVIEW OF THE LITERATURE

Very few publications are entirely devoted to cross-channel transfer of linear momentum and (or) to shear stress distribution. Most investigations into the determination of the shear stress in open channels were either directed toward methods of measuring shear stress or undertaken as a side product of a larger investigation. The major part of these investigations was done in conjunction with studies of sediment transport. This is partly due to the fact that a knowledge of the shear stress (or tractive force, as it is usually referred to in sedimentation studies) is required for investigation of channel stability.

Keulegan (1938), using the Kármán-Prandtl velocity law,

$$\frac{u}{u_*} = a + \frac{1}{\kappa} \ln \left(\frac{yu_*}{\nu} \right), \quad (4)$$

derived the expression for the mean velocity in a trapezoidal cross section

$$\frac{U}{u_*} = a - \frac{1}{\kappa} + \frac{1}{\kappa} \ln \left(\frac{R \bar{u}_*}{\nu} \right) + \frac{1}{\kappa} \beta - \bar{\epsilon} \frac{U}{\bar{u}_*} \quad (5)$$

in which

a = constant

R = hydraulic radius

u = velocity at a point

U = average velocity for the cross section

u_* = shear velocity, $\sqrt{\tau_0/\rho}$

\bar{u}_* = average shear velocity, $\sqrt{\bar{\tau}_0/\rho}$

y = distance above the channel bottom

β = correction for the variation in shear along the solid boundary

$\bar{\epsilon}$ = correction for apparent shear at the free surface

κ = Von Kármán's constant

ν = kinematic viscosity

Keulegan stated that the correction for apparent shear at the free surface may be neglected and that the correction for the variation in shear along the solid boundary of rectangular channels may be taken as 0.1. He showed that the hydraulic radius can be used in equation 5 as the characteristic length for the cross section. Using Bazin's data, Keulegan also computed the shear velocity for points along the bottom and walls of the channel by means of equation 5.

Lane (1955) made an attempt to determine the shear distribution by a mathematical process. He used the Kármán-Prandtl logarithmic distribution and boundary layer theory to obtain mathematical solutions of a supposedly analogous differential equation for a rectangular channel having a depth-to-width ratio of 1 to 2. His results showed a maximum shear stress on the bottom approaching $\gamma y_0 S_0$ (the two-dimensional shear stress) and a maximum of $0.76 \gamma y_0 S_0$ on the walls.

Leutheusser (1963), in a study of turbulent flow in rectangular ducts, determined the shear stress around the periphery of rectangular ducts having aspect ratios of 1 to 3 and 1 to 1. He computed the shear stress by use of Preston's technique. Leutheusser's tests were made at Reynolds numbers that ranged from 34,000 to 92,000. He found shear stress distribution to vary with Reynolds number.

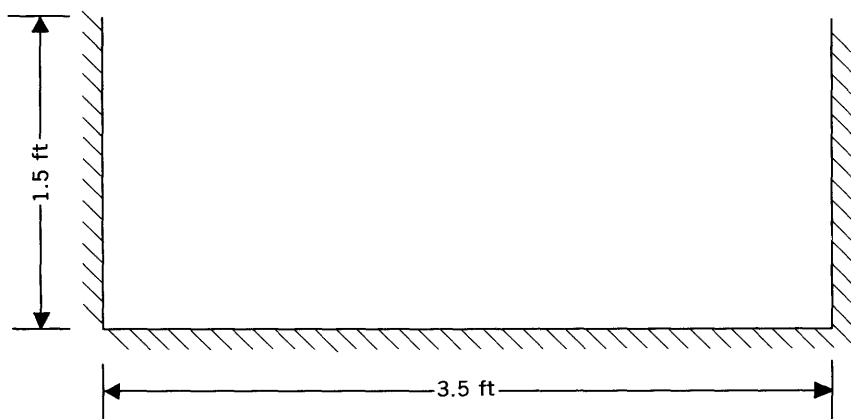
Hsu (1955) extended Preston's technique for the determination of local skin friction in pipes to that for boundary layer flow with adverse pressure gradients. He was able to check Preston's calibration curve almost identically for round-surface pitot tubes on flat surfaces that had either a zero pressure gradient or an adverse pressure gradient.

Hwang and Laursen (1963) showed that the methods evolved by Preston and Hsu give satisfactory results even for channels that have rough boundaries.

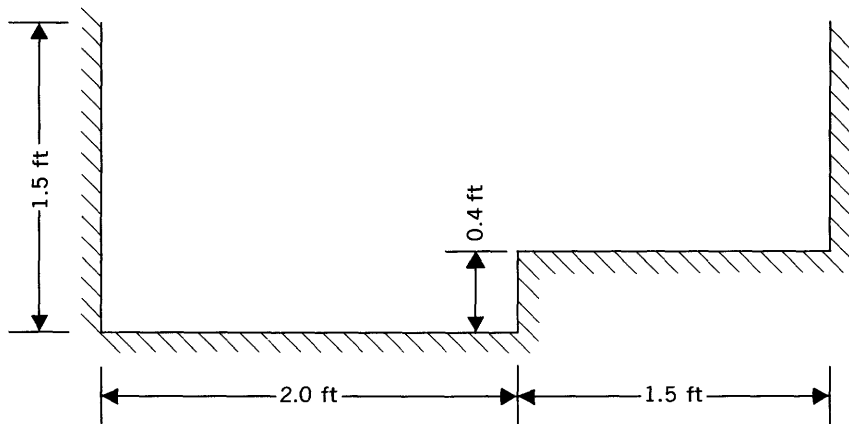
APPARATUS AND PROCEDURES

THE FLUME

The laboratory tests were made in a steel flume 3.5 feet wide, 18 inches deep, and 80 feet long (fig. 2). The flume is supported at its midpoint on a fixed pivot and at the ends by pairs of screw jacks. An electric motor at the pivot drives the two pairs of jacks simultaneously through torque tubes of equal length. The drive mechanism also furnishes a method for the determination of the flume slope. The number of turns made by the torque tubes from the level flume position is indicated by a mechanical counting device. The vertical displacement of the two ends of the flume for various counter readings



A



B

FIGURE 2.—Channel cross sections.

has been measured by precise levels. A calibration of counter reading against flume slope has been prepared from this data and from the measurement of the distance between the two end points. Tracy and Lester (1961) gave a detailed description of the flume.

Water is supplied to the flume by the laboratory recirculating system through either a 12- or a 6-inch line. Discharges are measured by a venturi meter in the 12-inch line, or by an orifice meter in the 6-inch line. Both meters were calibrated gravimetrically.

The depth of flow in the flume is regulated by an adjustable tailgate or by a sluice gate at the entrance of the flume.

Later, an overbank section was placed in this flume. The channel thus formed had a 2-foot-wide main flow passage and a 1.5-foot-wide overbank (fig. 2). These two sections were connected by a vertical wall 0.4 foot high. A rectangular channel 2 feet wide and 0.4 foot deep was then available.

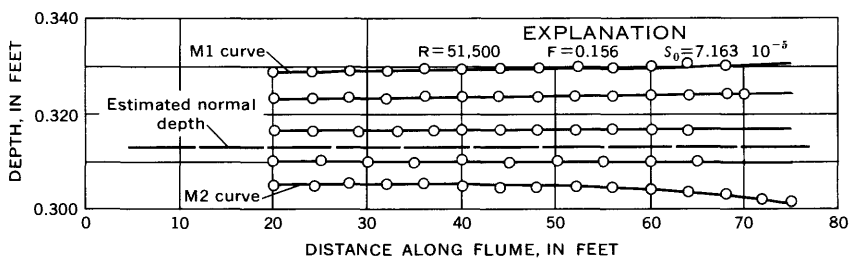
DEPTH MEASUREMENTS

Near the normal depth, flow in uniform channels varies gradually from section to section. The change may be almost imperceptible over short distances, as in the 80-foot length of the experimental flume. For mild channel slopes the normal surface profile is the upstream asymptote to the M1 and M2 backwater curves. For steep slopes the normal profile is the downstream asymptote to the S2 and S3 curves. In each profile the normal line lies between the two curves. The method used to determine the normal flow depth consisted of the measurement of the surface profile at depths slightly greater than the normal, and at depths just shallower than the normal. The normal depth was then interpolated between the two curves. Point-gage readings to the nearest 0.001 foot were made at five points in cross sections at 1-foot intervals for the length of the flume. The point-gage readings were compared with the piezometric level at selected points in the flume.

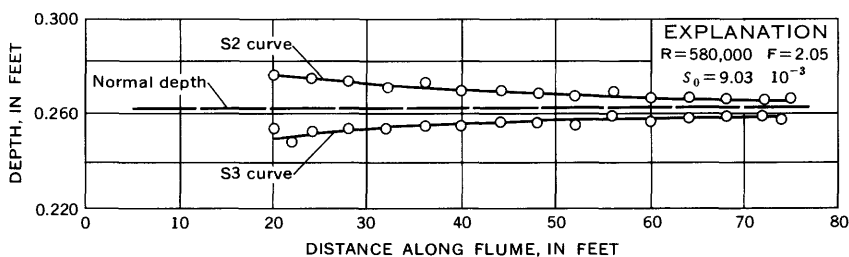
In figure 3 a typical set of depth measurements is shown for both a mild and a steep slope.

VELOCITY MEASUREMENTS

Point velocities were measured by means of a stagnation tube connected to a manometer, and floor piezometers connected to another



A



B

FIGURE 3.—Typical surface profiles.

manometer. The velocity data were taken at the downstream end of the flume near the 70-foot station (fig. 3). The stagnation tube was held in place by an arm on a carriage, which rolled on rails along the top of the sidewalls and could be locked in place anywhere along the flume. The carriage had a mechanism for precise positioning of the stagnation tube in both the horizontal and the vertical directions. The position of the stagnation tube, in relation to both the flume bottom and the vertical walls of the channel, could be determined to the nearest 0.0001 foot.

Point vertical velocity traverses were made in the flow at various locations in relation to the wall. A traverse was also made with the stagnation tube in contact with the wall.

RESULTS

This investigation utilized 22 tests in a 3.5-foot-wide channel and 4 tests in a 2-foot-wide channel. The pertinent information from each of these tests is listed in table 1.

TABLE 1.—*Summary of data*

| Test | B (ft) | U (fps) | y ₀ /B | $\gamma y_0 S_0$ (lb per sq ft) | R |
|------|-----------|------------|-------------------|------------------------------------|---------|
| 1 | 3.49 | 2.135 | 0.0752 | 0.02170 | 179,300 |
| 2 | 3.49 | 1.430 | .1142 | .01068 | 163,800 |
| 3 | 3.49 | 1.777 | .1152 | .01575 | 217,000 |
| 4 | 3.49 | 2.455 | .1182 | .02840 | 310,100 |
| 5 | 3.49 | 2.750 | .1198 | .03425 | 350,400 |
| 6 | 3.49 | 2.015 | .1422 | .02010 | 327,600 |
| 7 | 3.49 | 1.330 | .0616 | .00929 | 108,100 |
| 8 | 3.49 | 1.145 | .0287 | .00807 | 43,770 |
| 9 | 3.49 | 1.355 | .0424 | .01020 | 76,540 |
| 10 | 3.49 | .771 | .0424 | .00381 | 43,510 |
| 11 | 3.49 | 6.145 | .0978 | .14080 | 726,900 |
| 12 | 3.49 | 2.295 | .0284 | .02900 | 85,970 |
| 13 | 3.49 | 7.700 | .0532 | .22650 | 564,000 |
| 14 | 3.49 | 6.720 | .0550 | .17810 | 456,700 |
| 15 | 3.49 | 5.850 | .0559 | .14030 | 408,000 |
| 16 | 3.49 | 5.800 | .1012 | .13100 | 680,800 |
| 17 | 3.49 | 4.540 | .1030 | .08570 | 552,600 |
| 18 | 3.49 | 6.080 | .0740 | .14950 | 581,300 |
| 19 | 3.49 | 4.640 | .0800 | .08900 | 480,500 |
| 20 | 3.49 | 6.250 | .0263 | .17080 | 232,500 |
| 21 | 3.49 | 1.898 | .0868 | .01732 | 177,900 |
| 22 | 3.49 | 2.300 | .2115 | .02555 | 475,000 |
| 23 | 1.99 | 4.450 | .1156 | .23250 | 522,500 |
| 24 | 1.99 | 1.697 | .0740 | .01630 | 82,330 |
| 25 | 1.99 | 3.670 | .0489 | .06720 | 116,000 |
| 26 | 1.99 | 4.360 | .1975 | .03380 | 263,500 |

SHEAR-STRESS ANALYSIS

Two methods were used to determine shear stress at points along the channel periphery. The first method involved the use of the Kármán-Prandtl logarithmic law and the velocity data. The Kármán-Prandtl logarithmic law, including values of the constants established from Nikuradse's experiments (1950), is

$$\frac{u}{u_*} = 5.5 + 5.75 \log \frac{y u_*}{\nu} \quad (6)$$

Multiplying equation 6 by u_* and rearranging terms

$$u = 5.75 u_* \log y + \left(5.75 u_* \log \frac{u_*}{\nu} + 5.5 u_* \right) \quad (7)$$

in which $5.75 u_*$ is equal to the slope of the vertical velocity traverse curve (fig. 4). The shear stress can be determined because $u_* = \sqrt{\tau_0/\rho}$.

The second method used to determine the shear stress was Preston's method. This method was used for those tests in which the stagnation tube was placed in contact with the channel boundary. The first method was used only for the channel bottom. For the limited number of tests, data were available to make shear-stress determinations by both methods. The results compared favorably.

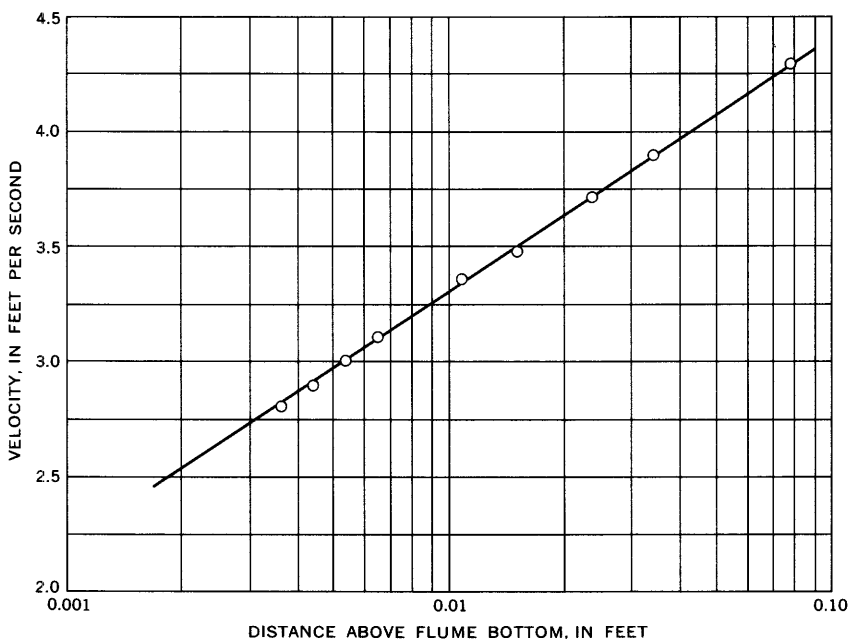


FIGURE 4.—Typical vertical velocity traverse (central region).

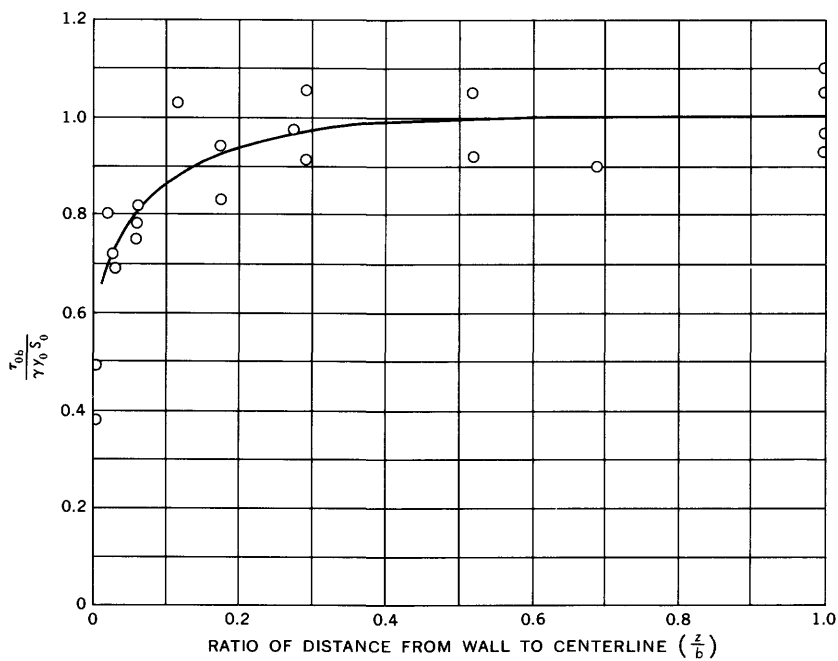
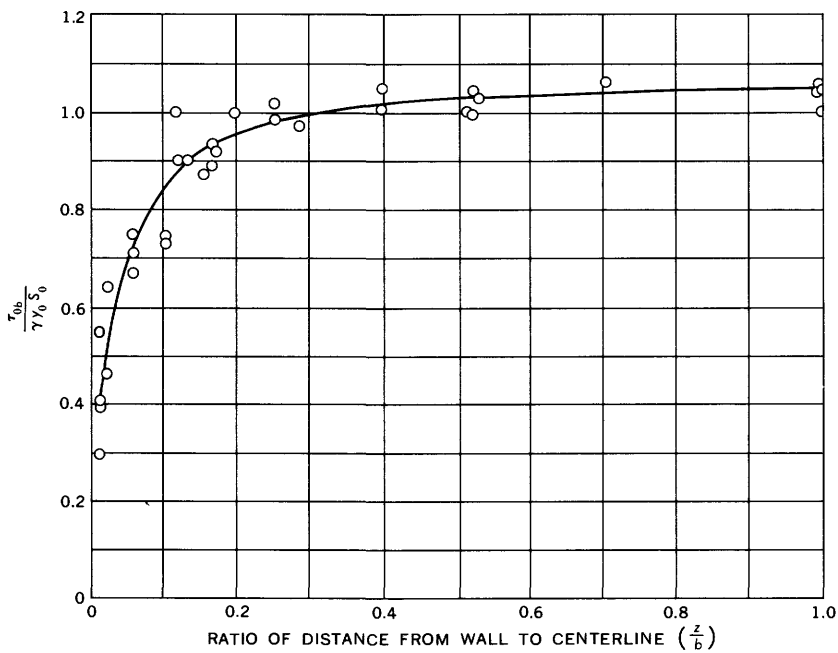
DISTRIBUTION OF THE SHEAR STRESS

Figures 5–11 show the shear-stress distribution across the channel bottom for a range of depth-to-width ratios. They represent the actual shear stress, $\tau_0 b / \gamma y_0 S_0$, divided by the two-dimensional shear stress as a function of z/b , which is the ratio of the distance from the vertical wall to the half-channel width.

These illustrations indicate that the shear-stress ratio decreases as the depth-to-width ratio increases. Thus, an increase in depth-to-width ratio beyond those values tested would probably result in still lower values.

Figure 12 shows the shear-stress distribution for channels whose depth-to-width ratio is 0.25 and 0.50, as presented by Lane (1955).

The shear-stress distribution for the vertical walls, for the different ranges of depth-to-width ratios, is shown in figures 13–17. The curves show the actual shear stress divided by the two-dimensional shear stress as a function of y/y_0 , which is the ratio of the point depth to the total flow depth.

FIGURE 5.—Shear-stress distribution, bottom ($0.026 < y_0/B < 0.030$).FIGURE 6.—Shear-stress distribution, bottom ($0.040 < y_0/B < 0.050$).

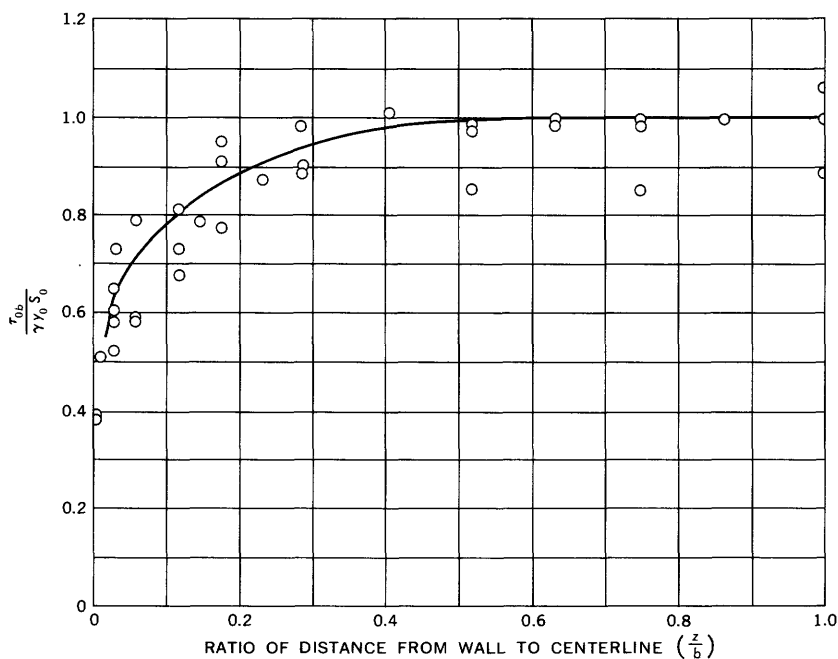


FIGURE 7.—Shear-stress distribution, bottom ($0.050 < y_0/B < 0.062$).

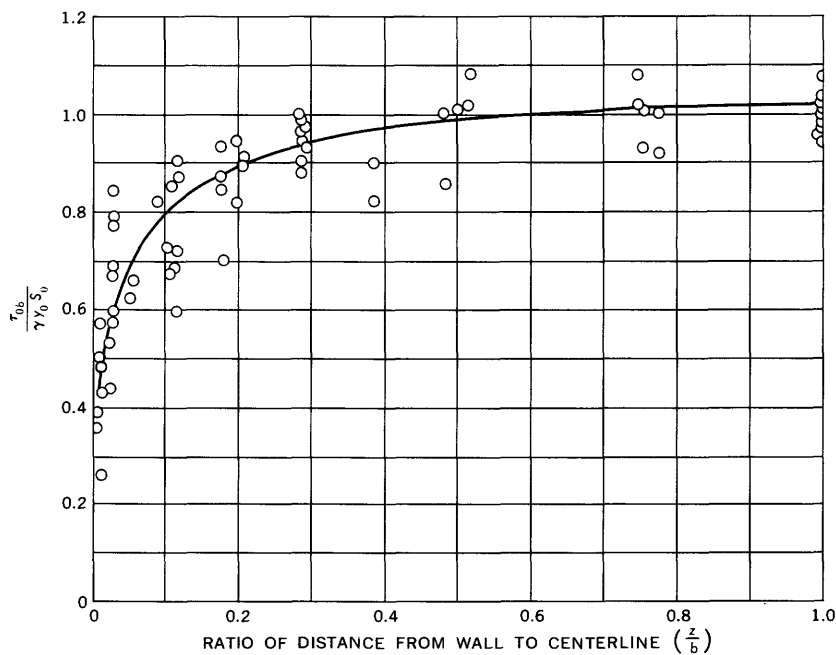
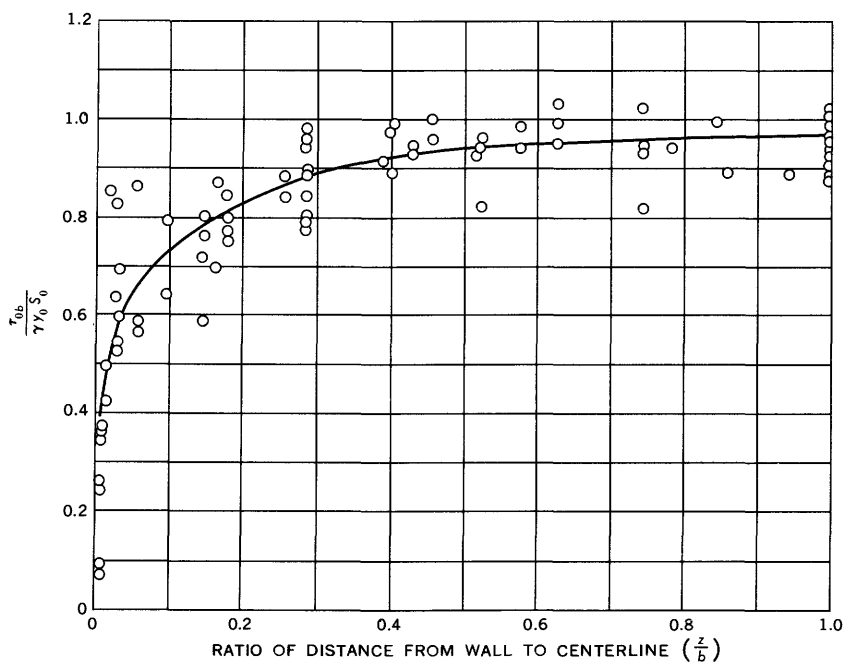
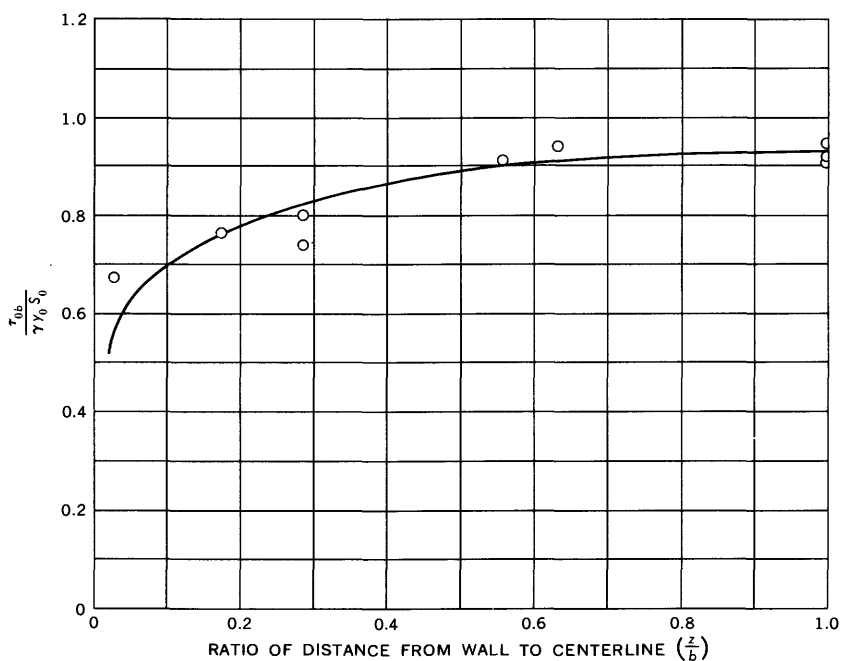


FIGURE 8.—Shear-stress distribution, bottom ($0.074 < y_0/B < 0.087$).

FIGURE 9.—Shear-stress distribution, bottom ($0.110 < y_0/B < 0.120$).FIGURE 10.—Shear-stress distribution, bottom ($0.140 < y_0/B < 0.145$).

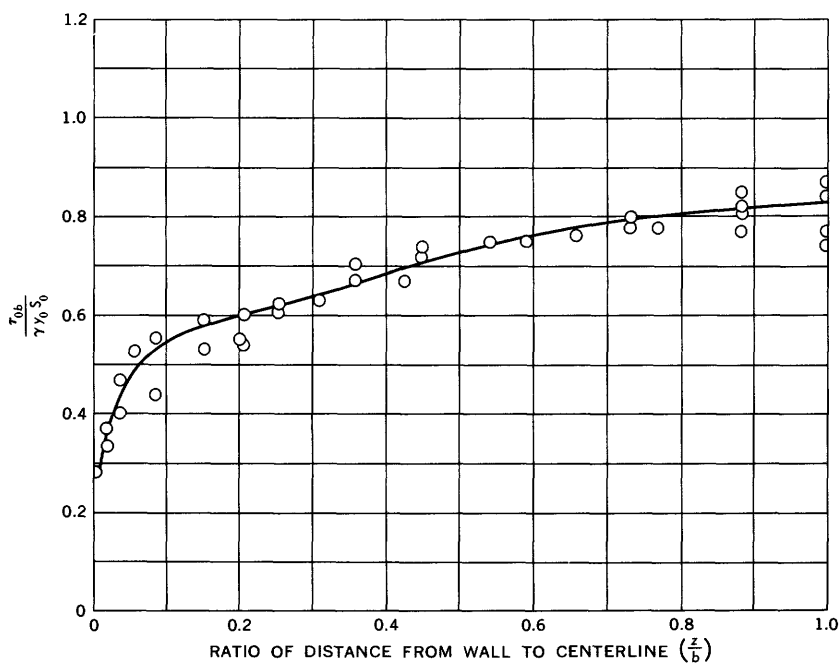


FIGURE 11.—Shear-stress distribution, bottom ($0.195 < y_0/B < 0.215$).

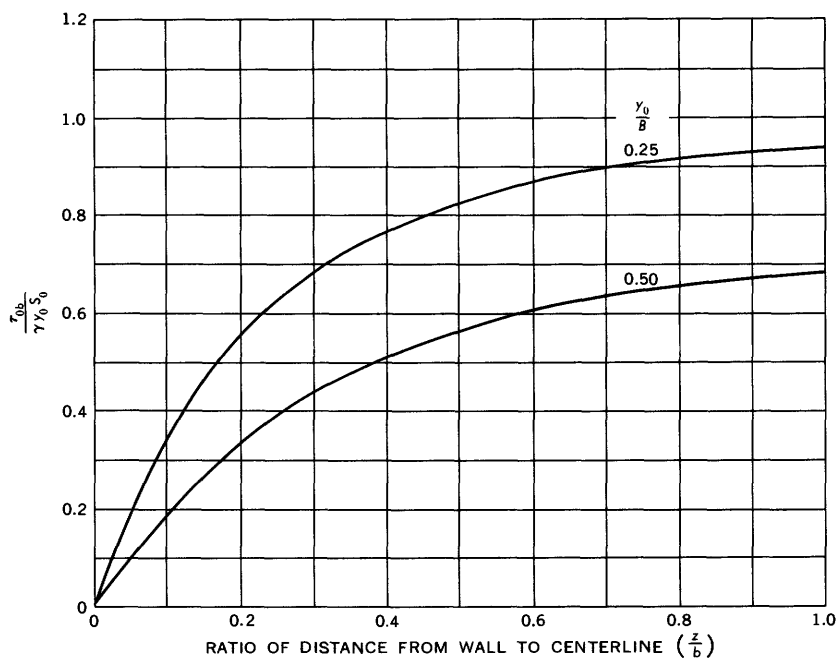
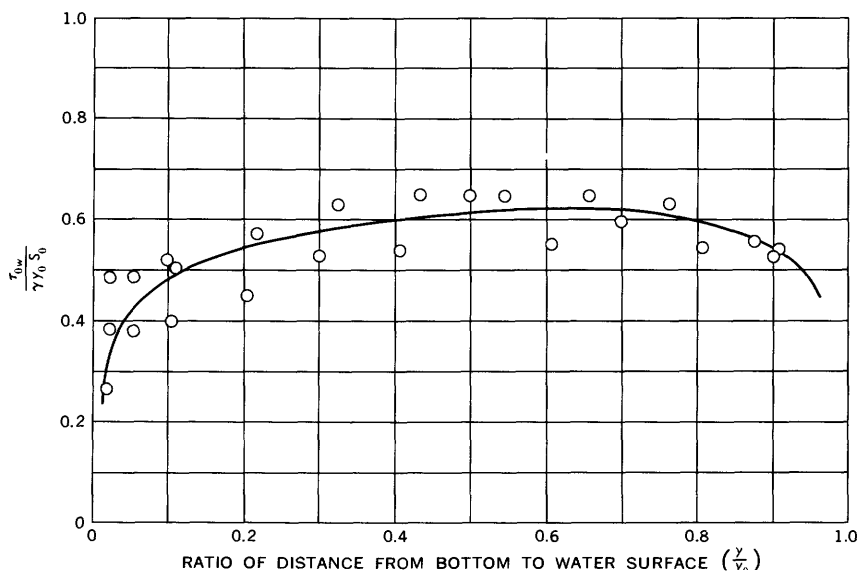
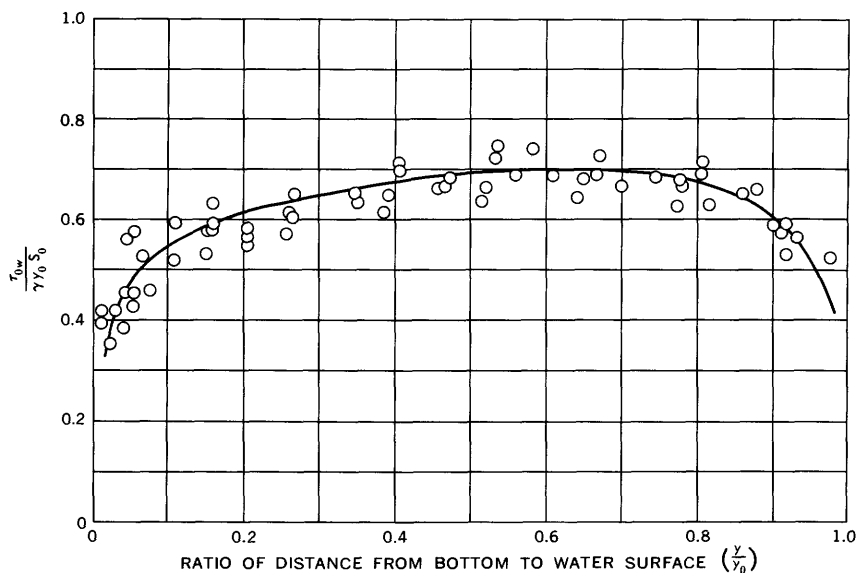


FIGURE 12.—Shear-stress distribution, bottom (Lane, 1955).

FIGURE 13.—Shear-stress distribution, wall ($0.026 < y_0/B < 0.030$).FIGURE 14.—Shear-stress distribution, wall ($0.040 < y_0/B < 0.062$).

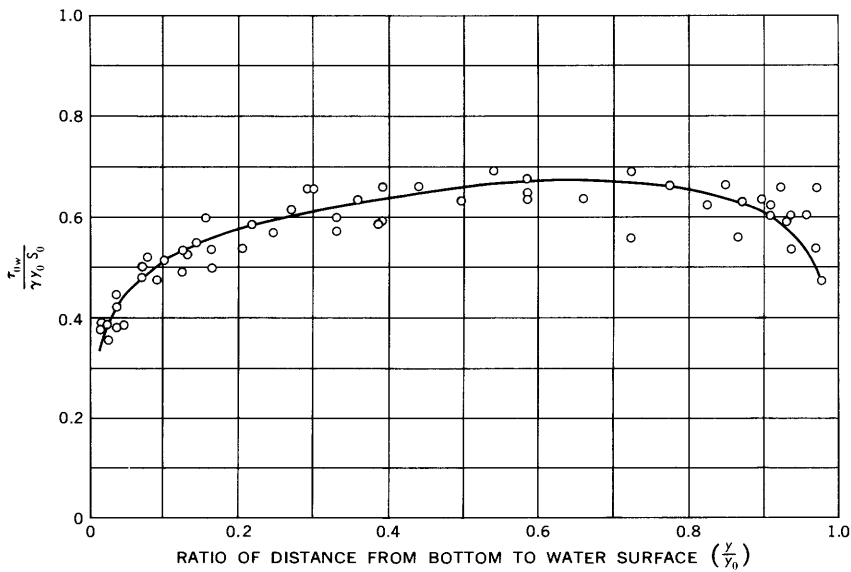


FIGURE 15.—Shear-stress distribution, wall ($0.074 < y_0/B < 0.087$).

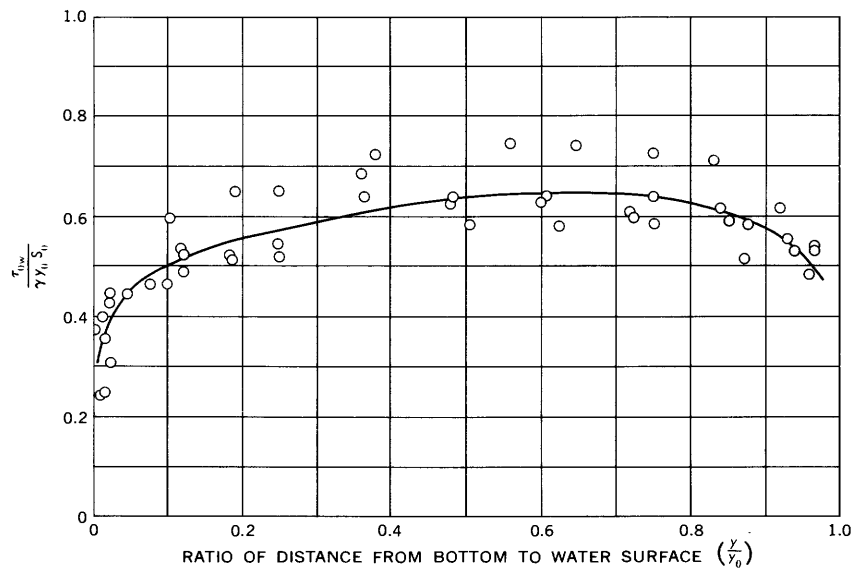


FIGURE 16.—Shear-stress distribution, wall ($0.110 < y_0/B < 0.120$).

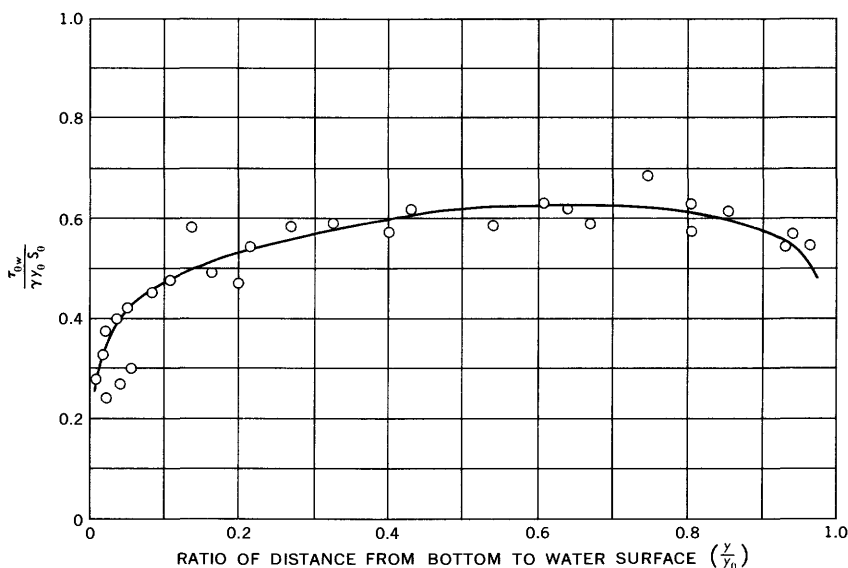


FIGURE 17.—Shear-stress distribution, wall ($0.140 < y_0/B < 0.215$).

MAXIMUM SHEAR STRESS

Figure 18 shows the maximum shear stress for the channel bottom, τ_{0b} (maximum), divided by the two-dimensional shear stress, $\gamma y_0 S_0$, as a function of the depth-to-width ratio of the channel cross section. The values of maximum shear stresses shown in figure 18 were obtained from figures 5–11 at $z/b=1.0$.

If the flow were two-dimensional the maximum shear stress, τ_{0b} (maximum), would be equal to $\gamma y_0 S_0$. From figure 18 one observes that the maximum shear stress, τ_{0b} (maximum), is equal to $\gamma y_0 S_0$ for values of y_0/B less than 0.08. The implication is that if the channel is narrower than the limit $y_0/B=0.08$, no two-dimensional flow zone exists. In other words, the width of the region affected by the wall is about six times the flow depth.

Tracy and Lester (1961) reported that, for the velocity distribution, the width of the wall region is two to three times the flow depth. They defined a wall region as the region which lies between the vertical wall and the vertical velocity traverse which first deviates from the characteristic logarithmic profile of the central region.

The central flow region defined by the shear-stress distributions is lesser in extent than that obtained using the criterion of Tracy and Lester. Another criterion such as the equality of turbulence characteristics would probably result in a third definition of a central flow region. A reasonable assumption is that no two-dimensional flow zone

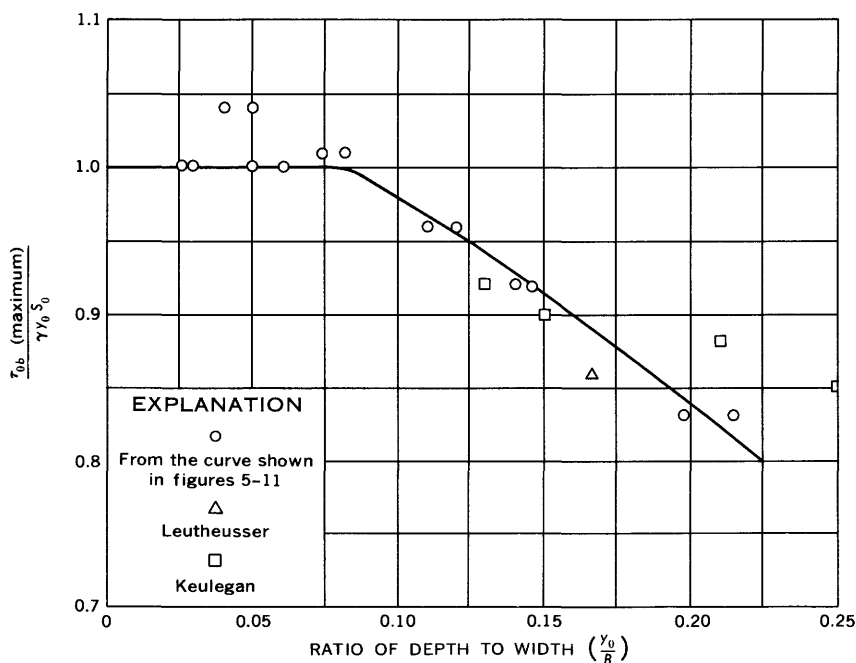


FIGURE 18.—Maximum shear stress, bottom.

exists in a rectangular channel; rather, the flow is approximately two-dimensional in the central regions of channels, in which $y_0/B < 0.08$.

Lane (1955) derived a curve, similar to that of figure 18, for the maximum shear stress on the channel bottom. Figure 19 is a comparison of the curve devised by Lane with the curve from figure 18, where the curve from figure 18 is extended to $y_0/B = 0.25$.

Figure 20 is a curve for the maximum shear stress on the walls, and figure 21 shows a curve, which was derived by Lane, for the maximum shear stress on the wall compared with the curve from figure 20.

Comparison of the mathematically derived curves with the curves computed from experimental data in figures 19 and 21 at $y_0/B = 0.25$ indicates that the mathematically derived curves give higher values of maximum shear stress, for both the bottom and the walls, than do the curves computed from experimental data. Comparison of figures 11 and 12 also shows that the values for the center of the channel given by the mathematically derived curve are higher than those computed from the experimental data.

The mathematically derived distribution is probably only a smooth-curve approximation of the actual shear-stress distribution, which

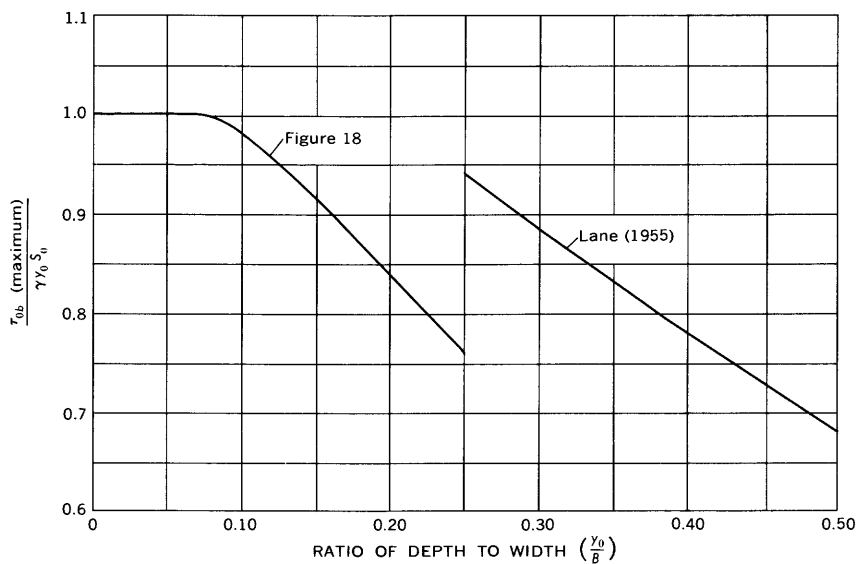


FIGURE 19.—Maximum shear stress, bottom.

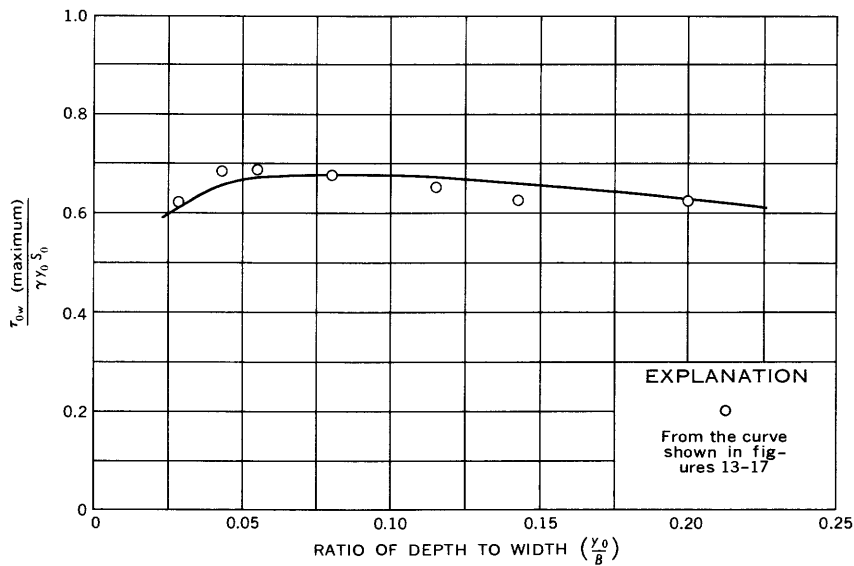


FIGURE 20.—Maximum shear stress, wall.

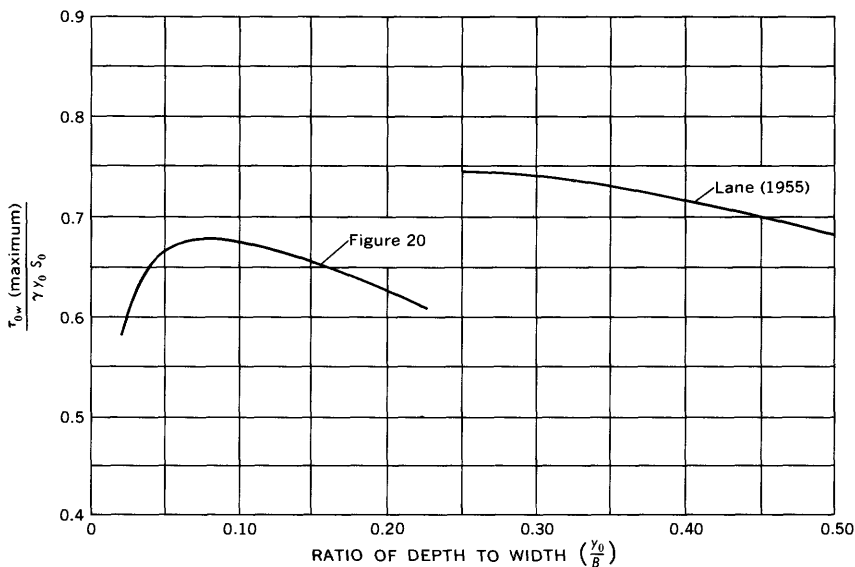


FIGURE 21.—Maximum shear stress, wall.

gives approximately the correct average shear stress but gives values for the maximum shear stress that are too high.

AVERAGE SHEAR STRESS

The average shear stress for the bottom and for the walls was determined by integrating the shear-stress distribution curves for each test. These average shear stresses, $\bar{\tau}_0$, divided by the two-dimensional shear stress, $\gamma y_0 S_0$, were then plotted in figure 22 as a function of the depth-to-width ratio, y_0/B , of the channel cross section. An average shear stress was found from the shear-stress distributions given by Keulegan (1938) and Leutheusser (1963). These values are also shown in figure 22.

A curve for the average shear stress for the entire channel boundary was computed by means of equation 8 (which was obtained by eliminating γS_0 from eq 3):

$$(B + 2y_0)\bar{\tau}_0 = (B)\bar{\tau}_{0b} + (2y_0)\bar{\tau}_{0w} \quad (8)$$

Figure 23 shows the curve computed from equation 8 compared with a curve for the average shear stress, for the total boundary of the cross

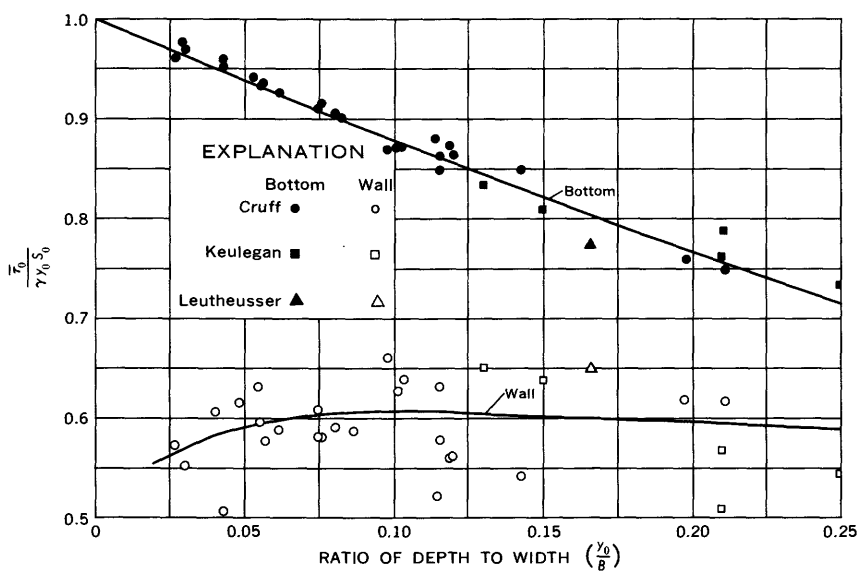


FIGURE 22.—Average shear stress.

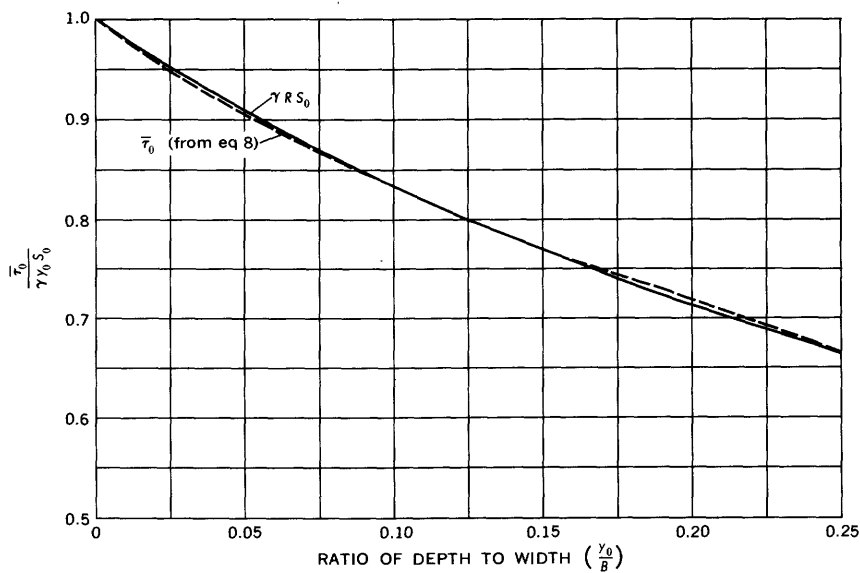


FIGURE 23.—Average boundary shear stress.

section computed by equation 3a. These two curves compare very closely. This would seem to indicate that the methods used in this report for computing shear stress gives satisfactory results.

APPARENT SHEAR FORCE

F'_a , the apparent shear force for an incremental distance, dx in the longitudinal direction, can be solved for by dividing equation 2,

$$-dx \int_0^b \tau_{0b}(-dz) - \tau_a y_0 dx + \gamma(b-z)(y_0 \sin \theta) dx = 0,$$

by dx and by rearranging terms. This results in the following equation:

$$F'_a = y_0 \bar{\tau}_a = \gamma(b-z)(y_0 \sin \theta) - \int_0^b \tau_{0b}(-dz). \quad (9)$$

The apparent shear force for an incremental distance, dx , was computed for the tests for various distances from the wall toward the channel centerline by use of equation 9. The uniform flow slope, S_0 , was substituted for $\sin \theta$. The shear stress across the channel bottom, τ_{0b} , was found from figures 5-11. The fluid specific weight, γ , the uniform flow depth, y_0 , the half-channel width, b , and the uniform flow slope, S_0 , were available, from the experimental data, for each test. Figure 24 shows the values of F'_a , the apparent shear force

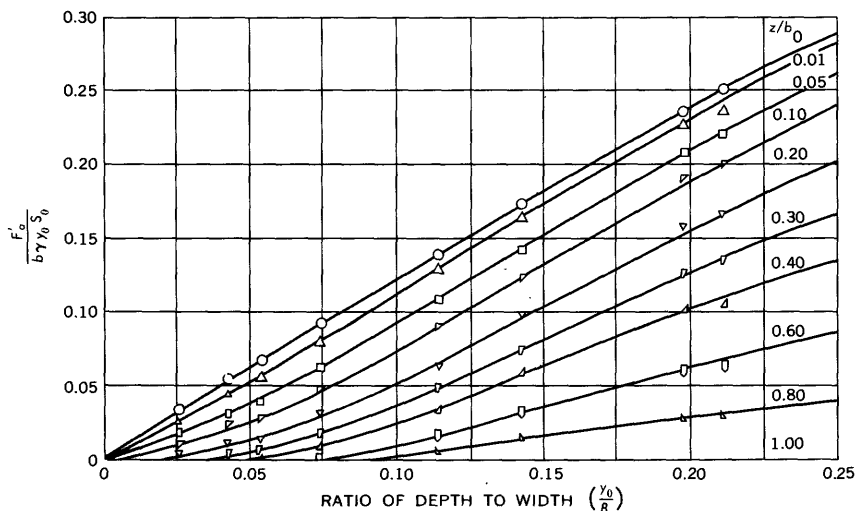


FIGURE 24.—Apparent shear force.

for an incremental distance, dx , divided by $b \gamma y_0 S_0$, as a function of the channel depth-to-width ratio, y_0/B , and of the ratio of the distance from the wall to the channel centerline, z/b .

CROSS-CHANNEL TRANSFER OF MOMENTUM

The cross-channel transfer of momentum, $\bar{\tau}_a y_0 dx$, can be found for uniform flow in a smooth rectangular open channel for any section between the wall and the channel centerline. This transfer for an incremental distance, dx , can be determined from figure 25 if the fluid specific weight, γ , the uniform flow depth, y_0 , the uniform flow slope, S_0 ,

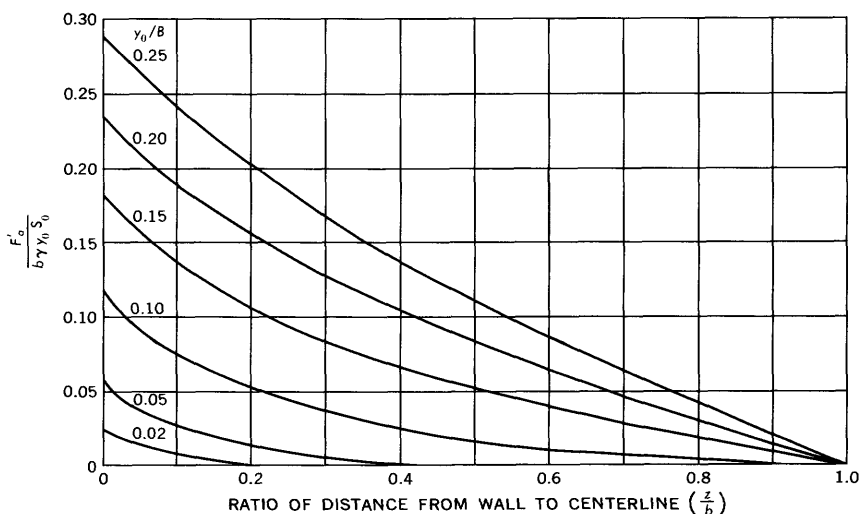


FIGURE 25.—Apparent shear force.

S_0 , and the half-channel width, b , are known.

Figure 25, which was derived from figure 24, shows curves, for various depth-to-width ratios (y_0/B), of F'_a (the apparent shear force for an incremental distance, dx) divided by $b \gamma y_0 S_0$, as a function of the ratio of the distance from the wall to the channel centerline (z/b).

SUMMARY

All shear flows are characterized by a net transfer of forward linear momentum from regions of higher linear momentum to regions of lower linear momentum.

In open channels there is also a lateral cross-channel transfer of linear momentum. This lateral transfer can be from a main channel section to an overbank section, or it can be from the central region to the vertical wall regions in a rectangular channel.

The object of this investigation was to study this lateral transfer of momentum from the central region to the vertical wall regions in smooth rectangular channels. The first step in the investigation was to determine the shear stress along the channel periphery. This shear stress was then used in the momentum equation to solve for the lateral cross-channel transfer of linear momentum.

The data used for this investigation were obtained previously and reported in part by Tracy and Lester (1961). The results of 26 tests were used. Test conditions covered a range of depth-to-width ratios from 0.026 to 0.211; Reynolds numbers, from 43,770 to 726,900; average channel velocity, from 0.77 to 7.70 feet per second; and two-dimensional shear stress, from 0.0038 to 0.2325 pounds per square foot.

The shear stress along the channel periphery was computed by two methods. One method made use of the Preston-tube technique, and the other, the Kármán-Prandtl logarithmic velocity law. From these computed shear stresses the shear-stress distributions, the maximum shear stress, and the average shear stresses for the channel bottom and walls were determined and plotted. The average shear stress for the channel bottom was much larger than that for the channel walls at the small depth-to-width ratios. The difference between the two shear stresses diminished as depth-to-width ratios increased. The depth-to-width ratio of the channel cross section was found to be the only flow characteristic which affected the boundary shear stress (distribution, maximum, and average) for smooth boundaries and for a moderate range of Reynolds numbers. Smooth rectangular channels having depth-to-width ratios less than 0.08 were found to have a central region in which shear stress is approximately equivalent to the shear stress for two-dimensional flow. In other words, for smooth rectangular channels the region in which the shear stress is affected by the wall extends a distance of about six times the flow depth laterally from the wall.

REFERENCES CITED

- Hsu, E. Y., 1955, The measurement of local turbulent skin friction by means of surface pitot tubes: U.S. Navy, David Taylor Model Basin, Research and Devel. Rept. 957, 18 p.
- Hwang, Li-San, and Laursen, E. M., 1963, Shear measurement technique for rough surfaces: Am. Soc. Civil Engineers, Hydraulics Div. Jour. v. 89, no. HY2, pt. 1, p. 19-37.
- Keulegan, G. H., 1938, Laws of turbulent flow in open channels: Natl. Bur. Standards Jour. Research, v. 21, p. 707-741.
- Lane, E. W., 1955, Design of stable channels: Am. Soc. Civil Engineers Trans., v. 120, p. 1234-1279.
- Laufer, John, 1951, Investigation of turbulent flow in a two-dimensional channel: Natl. Advisory Comm. for Aeronautics, TR-1053, 20 p.

- Leutheusser, H. J., 1963, Turbulent flow in rectangular ducts: Am. Soc. Civil Engineers, Hydraulics Div. Jour., v. 89, no. HY3, p. 1-19.
- Nikuradse, J., 1950, Laws of flow in rough pipes: Natl. Advisory Comm. for Aeronautics, TM-1292, 62 p.
- Prandtl, Ludwig, 1952, Fluid dynamics: New York, Hefner Pub. Co., p. 148-149 (translation by W. M. Deans).
- Rodriguez-Diaz, A. J., 1954, The hydraulic jump in a non-rectangular open channel: Atlanta, Ga., Georgia Inst. Technology unpub. M.S. thesis, 30 p.
- Tracy, H. J., and Lester, C. M., 1961, Resistance coefficients and velocity distribution, smooth rectangular channel: U.S. Geol. Survey Water-Supply Paper 1592-A, 18 p.
- Wilroy, R. D., 1953, An investigation of the critical depth in an open channel with a nonrectangular cross section: Atlanta, Georgia, Inst. Technology unpub. M.S. thesis, 41 p.